Materials Science and Engineering A 538 (2012) 53–57

Contents lists available at SciVerse ScienceDirect

Materials Science and Engineering A

journal homepage: www.elsevier.com/locate/msea

W–2 wt.%Y_2O_3 composite: Microstructure and mechanical properties

M. Battabyal*, R. Schäublin, P. Spätig, N. Baluc

Ecole Polytechnique Fédérale de Lausanne (EPFL), Centre de Recherches en Physique des Plasmas, Association Euratom-Confédération Suisse, 5232 Villigen PSI, Switzerland

ARTICLE INFO

Article history:
Received 25 October 2011
Received in revised form 4 January 2012
Accepted 5 January 2012
Available online 14 January 2012

Keywords:
Composites
Electron microscopy
Mechanical characterization
Sintering
Ductility

ABSTRACT

A W–2Y_2O_3 composite is produced by powder metallurgy, including the pressing of the mixed elemental powders, their sintering and hot forging. The microstructure of the obtained composite is investigated using light microscopy, scanning electron microscopy and transmission electron microscopy. It appears that the material is composed of W grains having a mean size of 1–2 μm and Y_2O_3 particles having a mean size of 300 nm to 1 μm. The W grains contain a high density of dislocations. The mechanical properties of this material are investigated using nanoindentation and 3-point bend test. Berkovich hardness value is found to be 4.9 GPa at 10 N load, which is similar to that of pure W. 3-Point bend test shows that the composite starts to show ductile behavior approximately at 400 °C and the bending stress continuously decreases from 200 °C to 1000 °C.

1. Introduction

Nowadays, fusion power reactor has drawn enormous attention as a future source of energy. However, it demands the availability of plasma facing materials that can withstand extreme conditions of temperature, irradiation and thermal stress. Pure tungsten (W) is considered as a well suited material for plasma facing applications due to its high melting point, high strength at high temperatures, good thermal conductivity, low thermal expansion coefficient, high sputtering threshold energy and limited activation under neutron irradiation [1–3]. Nonetheless, the use of W is limited because of its inherent low fracture toughness at all temperatures, associated with a high ductile-to-brittle transition temperature (DBTT), typically in the range from 300 to 600 °C. It has been found [4] that fine oxide particles strengthening (like La_2O_3) of W alloys emerged as potential structural materials in the modular helium cooled divertor concept of the near-term demonstration reactor DEMO. The poor DBTT and recrystallization temperature (RCT) values can be improved (by decreasing the DBTT and increasing the RCT) by adding fine oxide particles. In detail, the W precursors are blended with oxides and subjected to sintering and mechanical processing to achieve high densities. The DBTT and recrystallization temperature (RCT) of W–1%La_2O_3 under fusion neutron irradiation are estimated to be around 600 °C and 1300 °C, respectively. W alloys developed so far have an operating temperature window in the range from 800 to 1200 °C, as defined by their DBTT and recrystallization temperature [5]. However, for their use as structural material at low operation temperature, below 800 °C, and under fusion specific neutron irradiation, the material should exhibit a DBTT of about 200–400 °C, at least in the unirradiated condition.

Previous studies on W and its alloys at high temperature were devoted to analyze the evolution of mechanical properties with temperature and the determination of parameters that control the DBTT [6–9]. The present interest on these materials for fusion power reactor has led to new ways for improving these properties by dispersion hardening with thorium oxide (ThO_2) and lanthanum oxide (La_2O_3) [10] or Al–K–Si doping [4]. ThO_2-dispersed tungsten exhibits high mechanical strength at elevated temperatures, but its radioactive potential is an obstacle to practical application. La_2O_3-dispersed tungsten displays high creep resistance and improved tensile strength at high temperatures [4], but its hygroscopity limits its use [7]. It is reported that Y_2O_3 dispersed tungsten alloys enhances high temperature strength and creep resistance without any hazardous effect [11–13]. Hence, Y_2O_3 dispersed tungsten alloys appear to be a suitable material for plasma facing applications.

Very few work on the W–2Y_2O_3 composite has been reported so far [14–16]. The composite is mainly fabricated by hot isostaic pressing or spark plasma sintering and the mechanical property of the composite is not improved so far. In order to improve the mechanical property, we have fabricated W–2Y_2O_3 sample by a different powder metallurgy technique which is mainly by sintering of pressed W–2Y_2O_3 alloy powders followed by hot forging. The aim of this work is to investigate the microstructure and mechanical properties of this composite.

* Corresponding author. Tel.: +41 563102694; fax: +41 563104529.
E-mail address: manjusha.battabyal@psi.ch (M. Battabyal).

0921-5093/$ – see front matter
doi:10.1016/j.msea.2012.01.011

2. Experimental

A W–2Y_2O_3 sample was fabricated by pressing, sintering and hot forging in collaboration with the Plansee Company (Austria). A W–Y alloy powder with a mean particle size of 3.25 μm having 1.52% Y and 4482 ppm oxygen was pressed at ambient pressure. The pressed compact was sintered above 2000 °C in hydrogen atmosphere to get sample size of approximately 85 mm in diameter and 52 mm long. Then the sintered sample was hot forged to a diameter of 95 mm and to a length of 20 mm, corresponding to a deformation of about 75%. Finally the sample was stress relieved at Plansee Company.

Microstructure of the sample was examined using (i) Zeiss light microscope, (ii) scanning electron microscopy (SEM) using a focused ion beam/scanning electron microscope (FIB/SEM) device, the ZEISS NVision 40, operating up to 30 kV and (iii) transmission electron microscopy (TEM) using a JEOL 2010 microscope with a LaB_6 electron emittor and operated at 200 kV. For SEM and TEM, 3 mm discs were cut from the sample with a thickness around 400 μm. The disc was then ground using SiC papers with a grade from 800 to 4000 lubricated with water. For TEM, the disks were electrochemically thinned to electron transparency in a Tenupol-5 jet device from Struers Company using a chemical solution of 2 vol.% NaOH in water at room temperature and a voltage of 20 V.

Nanoindentation tests were performed using a nano-indenter G-200 from the MTS Company (USA) and a Berkovich tip, which is a three-sided pyramid. The ground 3 mm disc was glued on a sample holder and indentation is done with varying loads from 200 gf to 1000 gf in order to study the hardness as a function of load. The measurement was computerized using TestWork4 software.

For the 3-point bend test, rectangular rods 2 mm × 2 mm × 25 mm in size were cut from the sample by spark erosion. 3-Point bending tests were performed using a ZWICK 200 testing machine, in an argon flow, at temperatures ranging between room temperature to 1100 °C. Mini-bend bars, with dimensions of 2 mm × 2 mm × 25 mm, were used for the experiments, together with a specimen holder made of TZM, a molybdenum-based alloy.

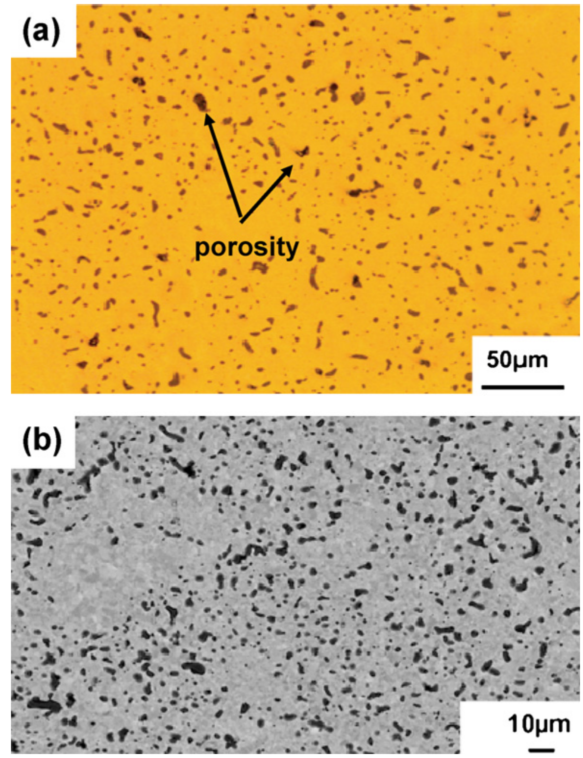

Fig. 1. (a) Light microscopy of the surface and (b) scanning electron microscopy of an electrochemically etched surface of W–2Y_2O_3.

Table 1
Average weight percent and atomic percent of yttria particles.

Element	Weight %	Atomic %
Y	21.4	60.2
O	78.6	39.8

3. Results and discussion

The W–2Y_2O_3 composite has low porosity relative to previously prepared W–2Y_2O_3 composite [14]. Light microscopy (Fig. 1a) enables to distinguish porosity from particles. From the Archimedes principle, the density of porosity is found to be about 0.7 vol.%. Scanning electron microscopy of W–2Y_2O_3 disk (Fig. 1b) shows that particles cover the surface inhomogeneously. X-ray energy dispersive spectroscopy (EDS) line scan performed in the SEM as shown in Fig. 2 shows the presence of Y and O in all the particles in a ratio corresponding to Y_2O_3. The size of the yttria particle varies from 300 nm to 1 μm. From the Image J analysis on the SEM images, we found that volume percent of Y_2O_3 phase in the bulk is 6.3%.

TEM bright field images of W–2Y_2O_3 are shown in Figs. 3 and 4. It is observed that the W-grains are larger than previously studied W–Y_2O_3 sample [14]. The average grain size in the studied sample varies between 1 and 2 μm where as average grain size of previously studied W–Y_2O_3 sample [14] is 500 nm. Few large yttria particles are found (Fig. 4). Note that during electro-polishing, some yttria particles may come out from the matrix. To confirm the composition of the yttria particles, EDS was carried out in the TEM on the particles (Table 1). The atomic percent of Y and O correspond well to yttria. The measured size of the Y_2O_3 particles is the same as the one measured in SEM, i.e. between 300 nm and 1 μm. The larger size of both tungsten grains and yttria particles may be due to the high sintering temperature.

The composite may have faced both solid phase and liquid phase sintering. On the one hand, solid phase sintering can occur as the sintering temperature is rather low for pure W, which is usually solid phase sintered at temperatures around 2000 °C [17]. On the other hand, in the case of W–2Y_2O_3 materials, liquid phase sintering can arise from (i) 0–0.304 at.% O–Y solid solutions melt in the range from 1522 to 1670 °C [18], (ii) eutectics of W–Y and W–Y_2O_3 form at 1522 °C [6] and 1560 °C [18], respectively, (iii) a $Y_2(WO_4)_3$ phase can form, which melts at 1440 °C [6] and (iv) the pseudo-binary phase diagram of the system WO_3–Y_2O_3 indicates that an eutectic phase forms at about 1160 °C [19]. However, liquid phase sintering was evoked as the most probable operating mechanism. All the abovementioned melting temperatures are well below the sintering temperature of 2000 °C that was used. Hence it may be suggested that by Ostwald ripening mechanism, yttria particles enter into the grains during pressing and increase in size during sintering. We found that there are few dislocations in the grains. These dislocations are most probably related to the thermal stresses generated during cooling from the sintering temperature [20]. As the fabrication process involves pressing, sintering and hot forging, the material undergoes various stresses internally as well as externally. The dislocations produced due to internal stress during sintering are influenced by the external forces during forging. These enhance the movement of the dislocations resulting to pile up of dislocations (Fig. 3(b)). At the grain boundary, these dislocations become more prominent as shown in the Fig. 3(a). The selected area electron diffraction (SAED) pattern in the grain shows the pattern corresponding to a ⟨1 1 1⟩ zone axis of the body centre cubic